ORIGINAL PAPER

A novel multipurpose device for guided knee motion and loading during dynamic magnetic resonance imaging

Nicholas M. Brisson[a,*]**, Martin Krämer**[b,c]**, Leonie A.N. Krahl**[a]**, Alexander Schill**[d]**, Georg N. Duda**[a,1]**,
Jürgen R. Reichenbach**[c,1]

[a] Julius Wolff Institute, Berlin Institute of Health at Charité - Universitätsmedizin Berlin, Germany
[b] Institute of Diagnostic and Interventional Radiology, Jena University Hospital, Friedrich Schiller University Jena, Germany
[c] Medical Physics Group, Institute of Diagnostic and Interventional Radiology, Jena University Hospital, Friedrich Schiller University Jena, Germany
[d] Research Workshop, Charité – Universitätsmedizin Berlin, Germany

Abstract

Introduction: *This work aimed to develop a novel multipurpose device for guided knee flexion-extension, both passively using a motorized pneumatic system and actively (muscle-driven) with the joint unloaded or loaded during dynamic MRI. Secondary objectives were to characterize the participant experience during device use, and present preliminary dynamic MRI data to demonstrate the different device capabilities.*

Material and methods: *Self-reported outcomes were used to characterize the pain, physical exertion and discomfort levels experienced by 10 healthy male participants during four different active knee motion and loading protocols using the novel device. Knee angular data were recorded during the protocols to determine the maximum knee range of motion achievable. Dynamic MRI was acquired for three healthy volunteers during passive, unloaded knee motion using 2D Cartesian TSE, 2D radial GRE and 3D UTE sequences; and during active, unloaded and loaded knee motion using 2D radial GRE imaging. Because of the different MRI sequences used, spatial resolution was inherently lower for active knee motion than for passive motion acquisitions.*

Results: *Depending on the protocol, some participants reported slight pain, mild discomfort and varying levels of physical exertion. On average, participants achieved ~40° of knee flexion; loaded conditions can create knee moments up to 27 Nm. High quality imaging data were obtained during different motion and loading conditions. Dynamic 3D data allowed to retrospectively extract arbitrarily oriented slices.*

Conclusion: *A novel multipurpose device for guided, physiologically relevant knee motion and loading during dynamic MRI was developed. Device use was well tolerated and suitable for acquiring high quality images during different motion and loading conditions. Different bone positions between loaded and unloaded conditions were likely due to out-of-plane motion, particularly because image registration was not performed. Ultimately, this device could be used to advance our understanding of physiological and pathological joint mechanics.*

Keywords: Dynamic MRI, Knee biomechanics, Multipurpose knee motion/loading device

1 Introduction

Magnetic resonance imaging (MRI) is a leading modality in the evaluation of musculoskeletal conditions due to its non-invasive, direct multi-planar capabilities and excellent soft tissue contrast at high spatial resolution [1]. However, musculoskeletal MRI is conventionally performed in static, unloaded positions that do not represent the actual dynamic physiology of joints [2–6] and may preclude detection of functional deficits. It is particularly relevant to evaluate musculoskeletal joint conditions in the context of motion and/or loading as deviations from normality can be intimately involved in the development and exacerbation of pathology and pain. For instance, altered joint mechanics resulting from anterior cruciate ligament injury/reconstruction are implicated in the onset and progression of knee osteoarthritis [7,8]. Similarly, abnormal patellofemoral kinematics is a risk factor for the development and progression of knee pain [9,10]. Therefore, in vivo measurements of joint motion and loading may play an important role in understanding physiological and pathological joint mechanics.

Use of dynamic MRI to quantify in vivo knee mechanics remains scarce; however, its application to study the knee joint during motion or under mechanical loading has increasingly shown promise in recent years [11,12]. In addition, the development of new dynamic MRI techniques, as well as specialized MRI-safe equipment to generate or guide knee motion and to impart mechanical loading onto the joint, facilitate the acquisition of valid and reliable data [11,13]. While various custom-made devices have been developed for this purpose, most allow for axial loading of the knee in a slightly flexed or fully extended fixed position by applying mechanical loads to the individual's foot via footplates or orthotic boots either passively using cable/pulley setups, elastic bands or ratcheting mechanisms, or actively using pneumatic actuators [12]. Alternatively, some devices/setups enable knee motion (passively or actively) without load application [11,13]; very few devices are multipurpose, enabling knee motion in combination with load application [14,15].

The scarcity of multipurpose devices is likely due to various logistical challenges that must be overcome: they must be built out of MRI-safe materials (i.e., non-magnetic, non-metallic, non-conducting) [16] and must fit and operate within the confines of the scanner bore. In particular, use of cumbersome and manually-operated components that extend from the scanner (e.g., cord and pulley systems) should be avoided to minimize the risk of equipment malfunction, MRI system damage or patient injury. Furthermore, such devices should allow for physiologically relevant magnitudes of joint motion and loading while ensuring patient comfort.

The purpose of this work was to develop a novel MRI-safe device for dynamic imaging of the knee joint that addresses the aforementioned challenges and that allows for guided knee motion in the sagittal plane, both passively (i.e., motor-driven) and actively (i.e., muscle-driven) with the joint loaded or unloaded. In this article, we describe the design and specifications of the knee motion/loading device; characterize the participant experience during active knee motion and loading using the device; and present preliminary data obtained from dynamic MRI to demonstrate the different capabilities of the device.

2 Material and methods

This study was approved by the research ethics boards of the Charité – Universitätsmedizin Berlin (EA2/088/16) and the Friedrich Schiller University Jena (4756-04/16). All participants provided written, informed consent prior to taking part in the study.

2.1 Device specifications

The knee motion/loading device (Figure 1) was specifically designed for a 3T whole-body MRI scanner with a 60 cm diameter bore (Magnetom Prisma Fit, Siemens Healthineers, Erlangen, Germany). The main components were built out of polyoxymethylene (POM), polylactic acid (PLA) filament, onyx filament and fiberglass, and the various parts were secured together using adhesives and nylon screws (see Appendix).

The different components of the device are depicted in Figures 2, 3 and 4; corresponding identifiers are given in square brackets in the following text. The baseplate [A] is composed of two overlapping, attached pieces. The proximal piece is single-plied (2.62 cm thick), sits atop the patient table, and has two cut-outs for the coil plugs [B] and four small pins on each side that can be pressed down into the slits of the patient table rails to secure the device in place. The distal piece is double-plied (3.16 cm and 2.62 cm thick) and sits atop the rails within the bore of the scanner, which are normally used to guide and support the patient table. The assembled baseplate (total dimensions of 170 cm x 54 cm) has an opening in its center through which the lower leg can move up and down, thus permitting a larger range of motion that is unhindered by the patient table.

Proximally, there are two pillow blocks [C] secured to the baseplate, each of which are connected to 30-toothed sprockets whose centers correspond to the axis of rotation of the knee. Each of these pillow blocks contains attachments in the front and on the sides for a thigh strap [D] and a rotary encoder [E], respectively. The encoder (MR338-Y10C10, Micronor, Camarillo, CA, USA) [F] – a fiber optic absolute position sensor with 0.025° resolution – connects to a remote controller module (MR330-1, Micronor, Camarillo, CA, USA) outside the MR room and enables real-time monitoring of knee flexion angles during MRI acquisition using a custom graphical user interface developed in MATLAB (MathWorks, Inc., Natick, Massachusetts, United States of America). A built-in thigh positioning wedge [G] lies between the proximal pillow blocks. A leg support [H] comprised of two rigid
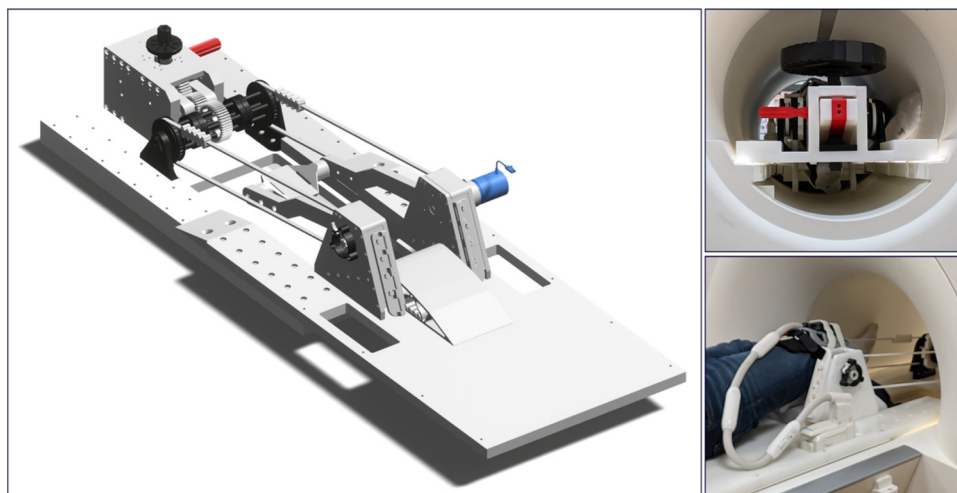
Figure 1. A 3D rendering of the knee motion/loading device (left) and two photographs of the device in a Siemens Magnetom Prisma Fit MRI scanner (right). The top right image (rear view) demonstrates how the distal part of the device sits atop the rails within the scanner bore, which are normally used to guide and support the patient table. The bottom right image (front, oblique view) demonstrates an individual positioned in the device with a flexible coil around the index knee, the thigh secured between the proximal pillow blocks and the ankle fastened to the leg support, as well as the coil plug setup.
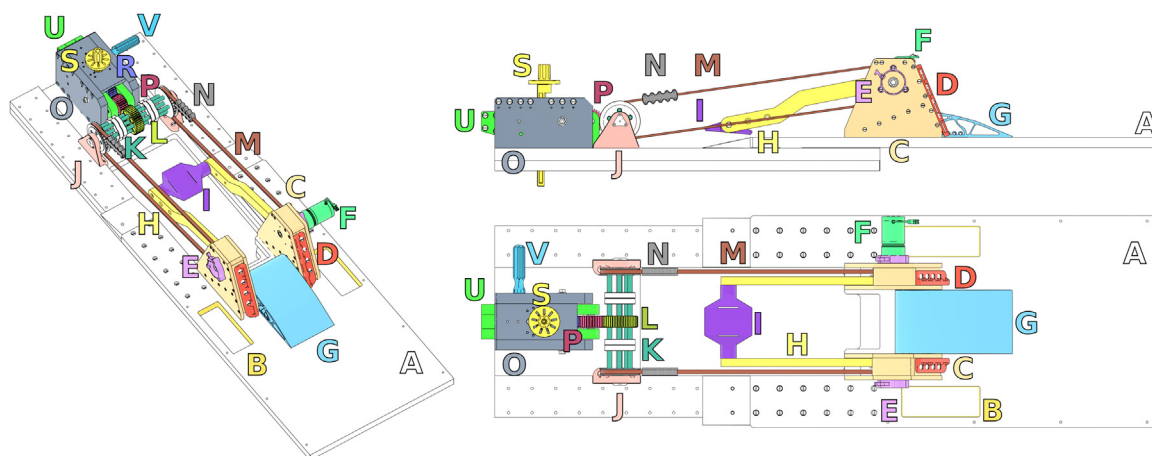

Figure 2. Depictions of the different components of the MRI-safe knee motion/loading device, including an oblique view (left), a side view (top right) and a top view (bottom right). The components, which are described in detail in the methods section, are as follows: baseplate [A]; cut-outs for coil plugs [B]; proximal pillow blocks (with 30-toothed sprockets) [C]; thigh strap attachments [D]; rotary encoder attachments [E]; rotary encoder [F]; thigh positioning wedge [G]; leg support [H]; ankle rest [I]; distal pillow blocks (with 30-toothed sprockets) [J]; drive axle [K]; 44-toothed circular gear [L]; belts [M]; belt clamps [N]; gearbox [O]; proximal, upper, 30-toothed circular gear [P]; proximal, lower, 30-toothed circular gear [Q] (not visible here; see Figure 3); distal 44-toothed circular gear [R]; 21-toothed linear gear [S]; weight plates [T] (not displayed here; see Figure 3); gearshift [U]; and locking pin [V].

shafts that run along either side of the lower leg (clearance of 16.3 cm between shafts) is connected proximally to the sprockets and protrudes from the pillow blocks; and distally by a foam-padded crosspiece that serves as an ankle rest [I]. The latter is adjustable to one of three positions (i.e., 33 cm, 38 cm, 43 cm) to accommodate different leg lengths.

Distally, there are two smaller pillow blocks [J] fixed to the baseplate, each of which are connected to 30-toothed

sprockets by the central shaft of a drive axle [K]. The drive axle is solidified by five peripheral shafts and four bracing disks, and contains in its center a 44-toothed circular gear [L]. The proximal and distal sprockets are linked by two 168.45 cm toothed belts [M] that run along either side of the lower leg, which are themselves secured by small clamps [N]. The most distal component of the device is the gearbox, which is used exclusively for active motion trials. For passive motion trials,
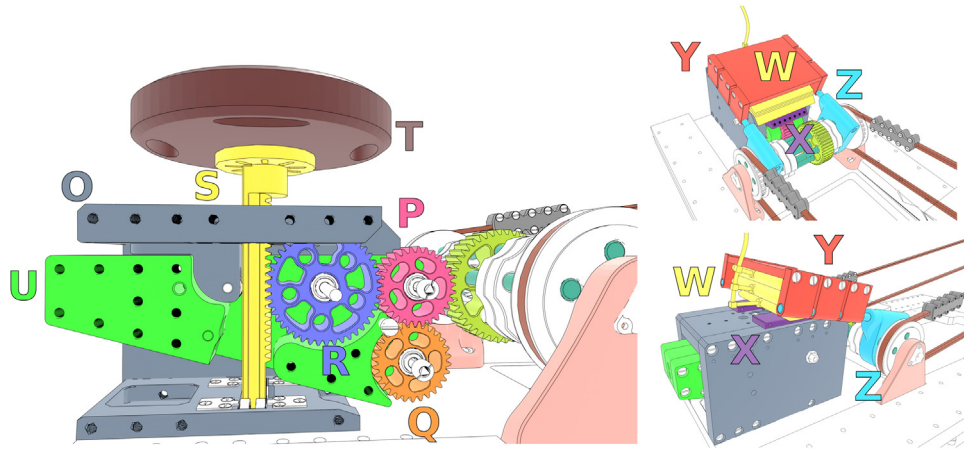
Figure 3. Close-up depictions of the different components that comprise the gearbox (left; cross-sectional view) and the air cushion setup (right) of the MRI-safe knee motion/loading device. The components are described in detail in the methods section. Components that are used exclusively for active motion trials are as follows: gearbox [O]; proximal, upper, 30-toothed circular gear [P]; proximal, lower, 30-toothed circular gear [Q]; distal 44-toothed circular gear [R]; 21-toothed linear gear [S]; weight plates [T]; gearshift [U]; and locking pin [V] (not displayed here; see Figure 2). Components that are used exclusively for passive motion trials are as follows: inflatable air cushions [W]; air cushion connector [X]; compression platform [Y]; and compression platform adapter [Z].

the gearbox is disabled and a motorized air pressure system is used to generate knee motion, as described subsequently.

2.1.1 Gearbox – active knee motion

For active motion trials, knee motion is guided by the belt and sprocket assembly that runs along either side of the lower leg and that connects to the gearbox, which is put into motion by the leg support when the participant actively flexes and extends the knee. The gearbox [O] is comprised of three interlinked circular gears: a proximal, upper, 30-toothed gear [P]; a proximal, lower, 30-toothed gear [Q]; and a distal 44-toothed gear [R] that interlinks with a 21-toothed linear gear [S], forming a gear rack upon which weight plates [T] can be placed to adjust the magnitude of knee loading. To enable the gearbox, one of its two proximal gears must be connected to the gear from the drive axle using a gearshift [U] and locking pin [V]: the selected configuration will determine the rotational direction of the gears and will depend on whether knee motion should be driven by the quadriceps or hamstring muscles.

Active motion trials can be performed in unloaded (no added weight) or loaded conditions, with up to 40 kg of external load. However, due to the various components implicated in generating knee motion (e.g., sprockets, belts), the actual load actively moved by the knee muscles is less than the applied external load. This linear relationship, which was determined experimentally with the ankle rest in the default middle position, can be expressed using the following equation: *load moved by knee muscles (kg) = 0.135 × external load (kg) + 0.943*. Thus, a maximum external load of 40 kg results in ~6.3 kg (or 62 N) applied to the muscles. Depending on the moment arm (i.e., distance from the knee axis of rotation and the adjustable ankle rest), the device can create knee moments

of ~20–27 Nm (without accounting for the inertial properties of the lower leg/foot).

2.1.2 Motorized air pressure system – passive knee motion

For passive motion trials, guided knee motion is generated using a motorized pneumatic system designed for slow and continuous motion over the available range, with speeds adjustable between ~1°/min and 10.5°/min. The motorized system can also be used to position and lock the knee in specific flexion angles for static imaging. To use the passive setting, three stacked, inflatable air cushions [W] are attached with an interlocking connector [X] atop the disabled gearbox of the device. A compression platform [Y], which is connected to the drive axle of the device via an adapter [Z], is positioned over the air cushions. Lastly, the air cushions are connected via a flexible air tube (20 m) to a motor assembly located outside the MR environment.

The motor assembly is powered by a 24 V power supply and is housed inside a control box [I]. A control panel [II] containing an organic light-emitting diode display and associated buttons (1.3" SPI Serial 128x64 OLED module for Arduino, SainSmart) is used to set the desired speed and range of motion. Passive knee motion is generated and controlled by a linear system, which is comprised of a microcontroller (Arduino Mega 2560, Arduino) [III], a digital stepper driver (DM542T, Stepperonline) [IV] and a modified electromechanical linear actuator (load capacity 750 N; stroke length 100 mm, Justech) with stepper motor (current 1.5 A; step angle 1.8°, MVPower) [V]. When activated, the actuator drives upward a piston rod [VI], which compresses a triad of inflatable air cushions [VII]. As the air cushions in the motor
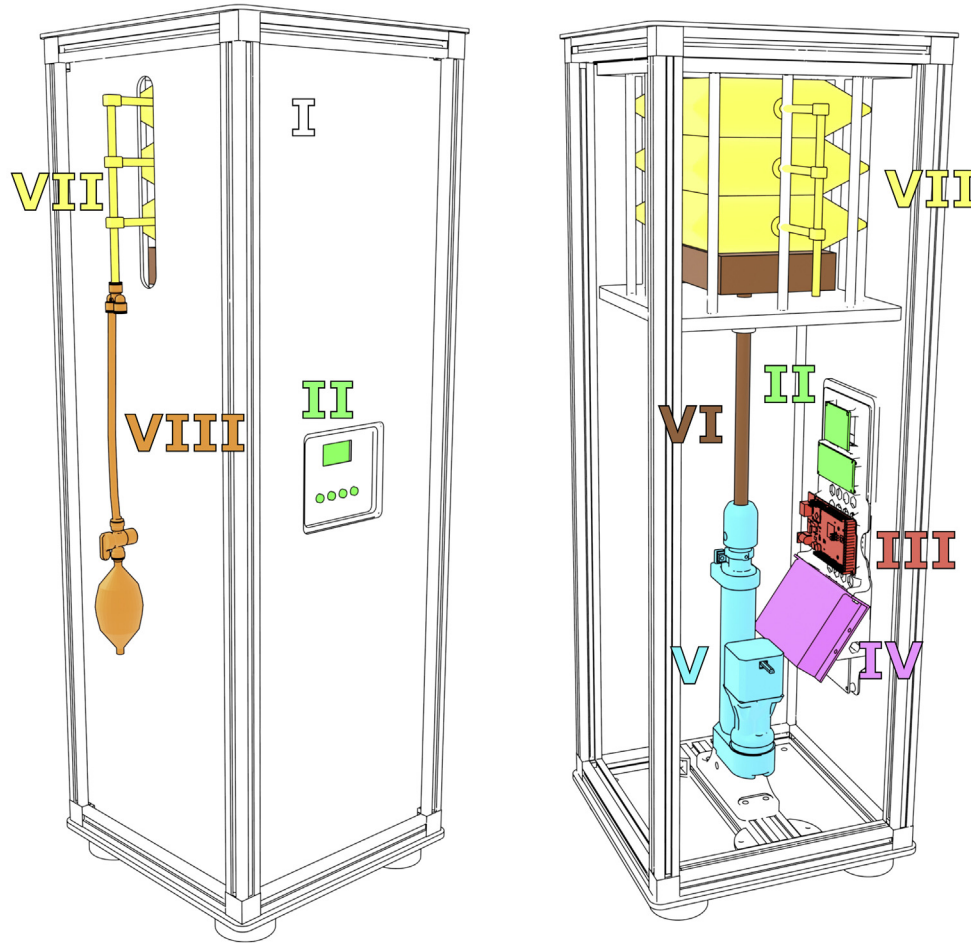
Figure 4. Depictions of the different components of the motor assembly used to generate passive motion with the MRI-safe knee motion/loading device, including an exterior view (left) and an interior view (right). The components, which are described in detail in the methods section, are as follows: control box [I]; control panel [II]; microcontroller [III]; digital stepper driver [IV]; linear actuator with stepper motor [V]; piston rod with compression plate [VI]; inflatable air cushions [VII]; and bulb air pump [VIII].

assembly are deflated, those attached to the device are inflated thereby raising the compression platform, rotating the drive axle and setting the device in motion, ultimately raising the lower leg. Reversal of this process (i.e., airflow in the opposite direction) will result in lowering of the compression platform and the lower leg. Finally, a manual bulb air pump [VIII] connected to the air cushions allows to equilibrate the air pressure in the system prior to a passive motion trial.

2.1.3 Participant positioning

The device can be used with either knee, in supine or prone position. The individual is positioned with the pelvis and lower limbs on the proximal portion of the baseplate and with the upper body extended onto the padded patient table. The index knee is instrumented anteriorly and/or posteriorly with one or two suitable flexible coils, and positioned between the two proximal pillow blocks with its axis of rotation aligned with that of the device using padding as required; the thigh is

fastened upon the wedge positioner; and the lower leg is fastened to the ankle rest approximately 2 cm proximal to the malleoli. The contralateral leg is placed alongside the bore. Once positioned, the participant is asked to perform several knee flexion-extension cycles to ensure that the leg is properly positioned within the device, and to ascertain whether there is any bodily discomfort during knee motion prior to data collection. Examples of a participant performing an active supine protocol, an active prone protocol, the transition into the bore, as well as passive motion using the motorized pneumatic system are shown in Video 1.

2.2 Participant experience during active knee motion and loading

Self-reported outcomes were used to characterize the experience of 10 healthy male participants (age 34.6 ± 6.0 years; body mass index $23.9 \pm 2.2 \, \text{kg/m}^2$), without prior lower-limb

injury/surgery or known musculoskeletal conditions, during four different active knee motion and loading protocols using the novel device. Each protocol consisted of a 90-second bout of active, cyclic knee flexion-extension over the available range of motion to the beat of a metronome. The protocols were as follows: (1) 4 cycles/min with 20 kg of external load; (2) 6 cycles/min with 20 kg of external load; (3) 4 cycles/min with 35 kg of external load; and (4) 6 cycles/min with 35 kg of external load. Participants were in supine position and the device gears were configured for quadriceps-driven motion, resulting in concentric contractions with knee extension and eccentric contractions with knee flexion. The protocols, which were completed outside the MR environment using a specialized setup that emulated the physical constraints of the scanner bore, used knee motion speeds realistic for dynamic MRI (i.e., to accommodate data sampling rate) and external loads that produced physiologically relevant knee loading magnitudes. Knee angular data were recorded with the rotary encoder during the protocols to determine the maximum knee range of motion achievable.

After completing each protocol, participants answered the questions "How much pain did you experience (and where)?" and "How physically exerting was the task?" using an 11-point numerical rating scale ranging from 0 "none/not at all" to 10 "extreme(ly)". Participants also answered the question "How much discomfort did you experience (and where)?" using a Likert scale with the following five mutually exclusive answer options: not uncomfortable; barely uncomfortable; somewhat uncomfortable; very uncomfortable and extremely uncomfortable. These questions were deemed valuable in determining whether it would be feasible to extend the use of the knee motion/loading device to persons with musculoskeletal knee conditions who may experience worsening symptoms with motion and loading.

2.3 Magnetic resonance imaging data acquisition

Knee MRI scans were acquired for three volunteers without prior lower-limb injury/surgery, known musculoskeletal conditions or contraindication to MRI. These volunteers were not part of the aforementioned group that completed the knee motion and loading protocol. Dynamic MRI was performed using a 3T whole-body Magnetom Prisma Fit scanner (Siemens Healthineers, Erlangen, Germany) and, depending on the desired knee coverage, one or two multipurpose flex coils each with eight receive channels (Variety, NORAS MRI products GmbH, Höchberg, Germany). To demonstrate the different capabilities of the knee motion/loading device, three distinct MRI measurements were performed: i) two-dimensional (2D) imaging of unloaded, passive knee motion; ii) three-dimensional (3D) imaging of unloaded, passive knee motion; and iii) 2D imaging of unloaded and loaded, active knee motion.

Dynamic 2D imaging was acquired for one volunteer (male, 29 years old, 70 kg) in supine position during a passive knee extension-flexion cycle. Data were collected continuously over 9 minutes using one flex coil positioned anteriorly and a vendor-supplied 2D multi-slice Cartesian turbo spin-echo (TSE) sequence with the following parameters: (0.5 x 0.5 x 3.0) mm^3 voxel size, 405 Hz/pixel acquisition bandwidth, echo time (TE) of 106 ms, repetition time (TR) of 780 ms, 150° refocusing flip angle and 5 sagittal slices, resulting in a temporal resolution of 7.8 s per frame. Subsequently, a second passive knee extension-flexion cycle was performed over 9 minutes to acquire data with enhanced soft tissue contrast using a custom 2D single-slice radial gradient recalled echo (GRE) sequence [17] with the following parameters: (0.6 x 0.6 x 4.8) mm^3 voxel size, 1929 Hz/pixel acquisition bandwidth, 2.46 ms and 7.48 ms TE, 15 ms TR, 12° excitation flip angle, a single sagittal slice and golden-angle temporal ordering of the radially rotated readouts [18], resulting in a temporal resolution of 7.7 s per frame. The radial GRE sequence used fat saturation before every excitation pulse; the Cartesian TSE sequence did not. For both sequences, the focus was to acquire high-resolution 2D sagittal slices by leveraging the slow, continuous, passive motion achievable with the device.

Dynamic 3D images with isotropic resolution were acquired for one volunteer (male, 31 years old, 65 kg) in supine position during one passive knee extension-flexion cycle. Data were collected continuously over 48 minutes using one flex coil positioned anteriorly and a 3D ultra-short echo time (UTE) imaging sequence [19] with the following parameters: (1.2 x 1.2 x 1.2) mm^3 voxel size, 1240 Hz/pixel acquisition bandwidth, 0.05 ms TE, 2.0 ms TR, 5° excitation flip angle and fat saturation before every tenth excitation pulse, resulting in a temporal resolution of 88 s per frame. In contrast to the dynamic TSE and GRE sequences used in the previous measurement, the UTE sequence also obtains signal in tissues with short T_2^* such as tendons and ligaments [20]. The UTE sequence was also selected because its center-out 3D radial nature renders it very robust against motion and aliasing artifacts [21].

Dynamic 2D imaging was acquired for one volunteer (female, 28 years old, 60 kg) in supine position as several knee extension-flexion cycles were actively performed over the available range of motion to the beat of a metronome (2 cycles/min). The device gears were configured for quadriceps-driven motion, eliciting concentric contractions with knee extension and eccentric contractions with knee flexion. The knee motion speed was selected to accommodate the MRI data sampling rate. MRI data were collected continuously over 2 minutes using two flex coils positioned anteriorly and posteriorly, respectively, and 2D single-echo, radial GRE imaging with a golden-angle temporal order scheme and the following parameters: (1.6 x 1.6 x 4.8) mm^3, 2893 Hz/pixel acquisition bandwidth, 2.4 ms TE, 5.1 ms TR, 10° excitation flip angle and a single sagittal slice. The image acquisition was performed twice; first without load and then with an applied external load of 15 kg. Knee angular data were recorded simultaneously
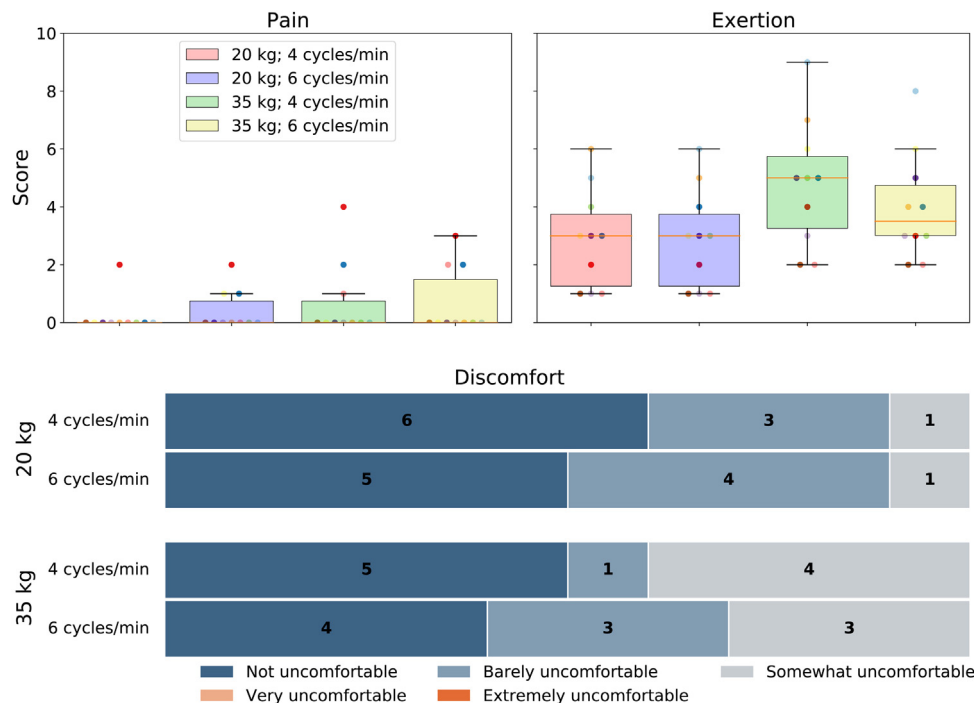
Figure 5. Self-reported outcomes characterizing the experience of 10 male participants who completed four different protocols using the knee motion and loading device. Each protocol consisted of a 90-second bout of active (i.e., quadriceps-driven), cyclic, knee flexion-extension over the available range of motion to the beat of a metronome. Pain and physical exertion were rated from 0 "none/not at all" to 10 "extreme(ly)". Physical discomfort was rated using a Likert scale with five mutually exclusive answer options.

with the rotary encoder. Images were reconstructed using nonlinear inverse reconstruction [22,23] after binning the radial MRI readouts retrospectively into $1°$ windows based on the measured knee angles.

Cartesian TSE images were reconstructed online at the scanner using the vendor-supplied reconstruction pipeline. The 2D and 3D radially-acquired datasets were reconstructed offline with MATLAB using re-gridding with iterative sampling density compensation and an optimized kernel [24]. No image registration between frames was performed.

3 Results

3.1 Participant experience

The self-reported outcomes characterizing the experience of the 10 participants who completed the active knee motion/loading protocol are presented in Figure 5. Slight pain was reported by one participant for the protocol with the lowest speed and lowest external weight (4 cycles/min; 20 kg), and by three participants for all other protocols. Furthermore, mild physical discomfort was reported by four to six participants depending on the protocol, while varying levels of physical exertion were reported by all participants for all protocols. All pain and discomfort were reported in the anterior aspect

of the index thigh (i.e., quadriceps), with the exception of one instance when discomfort was reported in the buttock (6 cycles/min; 20 kg). The mean ± standard deviation maximum knee range of motion achieved actively was $39.5° ± 3.4°$ (minimum: $31°$; maximum: $44°$), which varied depending on the length of the lower leg/foot and ankle position (plantar/dorsiflexed).

3.2 Magnetic resonance imaging data

High-resolution 2D MRI scans acquired in sagittal orientation during slow, passive knee motion are displayed in Figure 6. All images were free of motion artifacts, indicating that the temporal resolution was sufficient to resolve the motion. With the knee near full extension, the Cartesian TSE sequence showed minor streaking artifacts in some posterior knee muscles, likely caused by aliasing from tissues that moved outside the field-of-view. The radial T_1-weighted GRE sequence did not exhibit any aliasing artifacts because of the twofold readout oversampling of the k-space data and provided images with high cartilage contrast and residual signal in the patellar tendon.

Dynamic 3D data acquired with a UTE sequence during slow, passive knee motion are shown in Figure 7. Due to the isotropic spatial resolution, dynamic images could be retrospectively extracted from arbitrarily oriented slices.
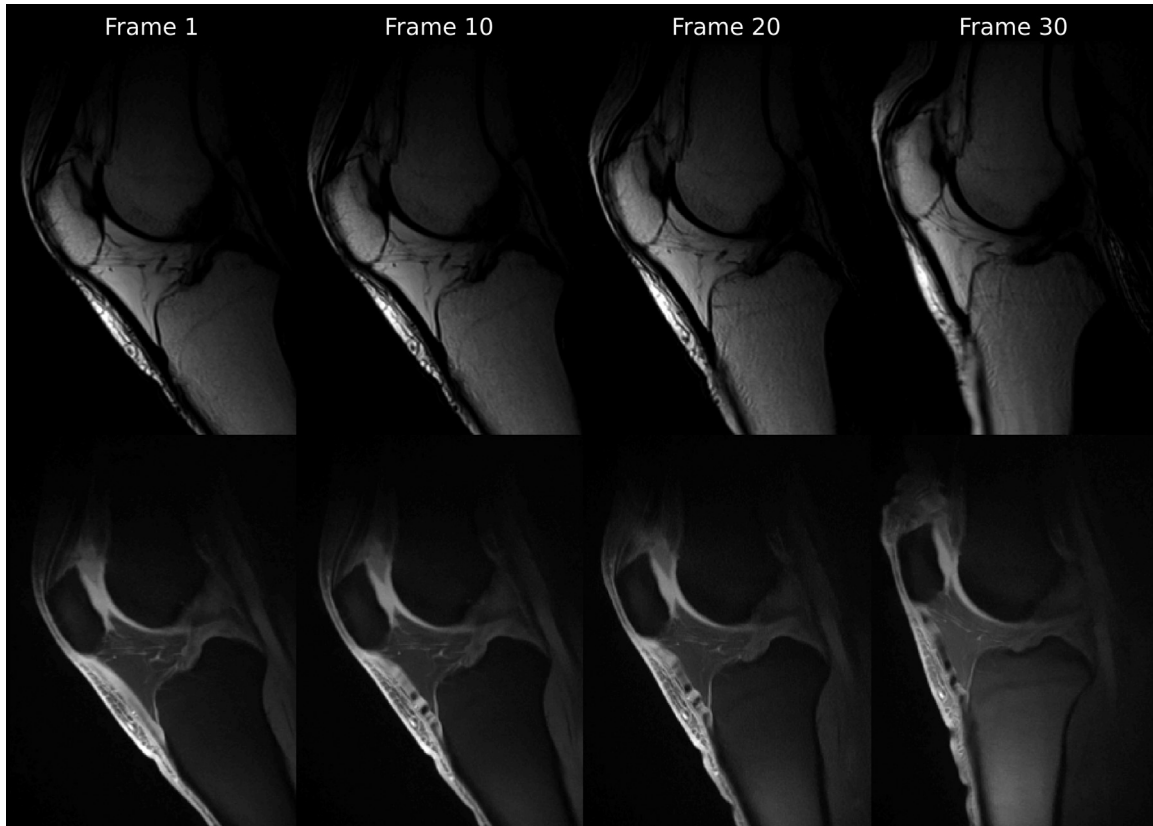
Figure 6. Four selected frames illustrating the extension portion of one passive knee extension-flexion cycle acquired in the sagittal plane. High-resolution images were acquired continuously over 9 minutes with 2D multi-slice TSE without fat saturation (top row) and 2D single-slice GRE with fat saturation (bottom row) imaging sequences. Videos showing all frames acquired continuously are available (Videos 2 & 3).

Image contrast was also T_1-weighted (as in the aforementioned 2D GRE sequence), but with additional signal in tissues with very short T_2^* relaxation times (i.e., tendons, ligaments).

Fast 2D sagittal MRI scans and knee angular data acquired during active knee motion are presented in Figure 8. Use of a 1° knee angle window for image reconstruction resulted in images with sufficient temporal and spatial resolution to present the active knee motion without artifacts (i.e., no major blurring or streaking). However, these images had inherently inferior spatial resolution compared to those from the passive motion acquisitions due to the faster knee motion speed. Visual comparison of the scans acquired for the loaded and unloaded conditions showed slightly different positions for the femur, tibia and patella in the through-plane direction, likely due to out-of-plane motion, particularly because image registration was not performed. In addition, less knee extension was achieved during the loaded condition than for the unloaded condition, reflecting either natural variability in knee motion between cycles or an inability to adequately contract the knee extensor muscles and fully straighten the leg under the given load.

4 Discussion

In this work, we described the design and specifications of a novel multipurpose device for guided knee motion and loading during dynamic MRI. This device addressed various logistical challenges, including use of MRI-safe materials, operating within the confines of a closed scanner bore, and allowing for physiologically relevant magnitudes of joint motion and loading [25]. Moreover, self-reported outcomes demonstrated that the use of the device was generally well tolerated in healthy adult men. Finally, device functionality and suitability for use with dynamic MRI was demonstrated through various types of acquired data. Use of such multipurpose devices for acquisition of in vivo measurements of knee motion and loading may provide valuable insight into physiological and pathological joint mechanics.

The device operated within the 60 cm diameter closed bore of the MR scanner and allowed for knee motion between ∼0° (full extension) and ∼40° of flexion, with joint moments up to ∼27 Nm during volitional motion. The attained knee range of motion was ∼10° greater than for previously reported multipurpose devices, likely due to the opening in the
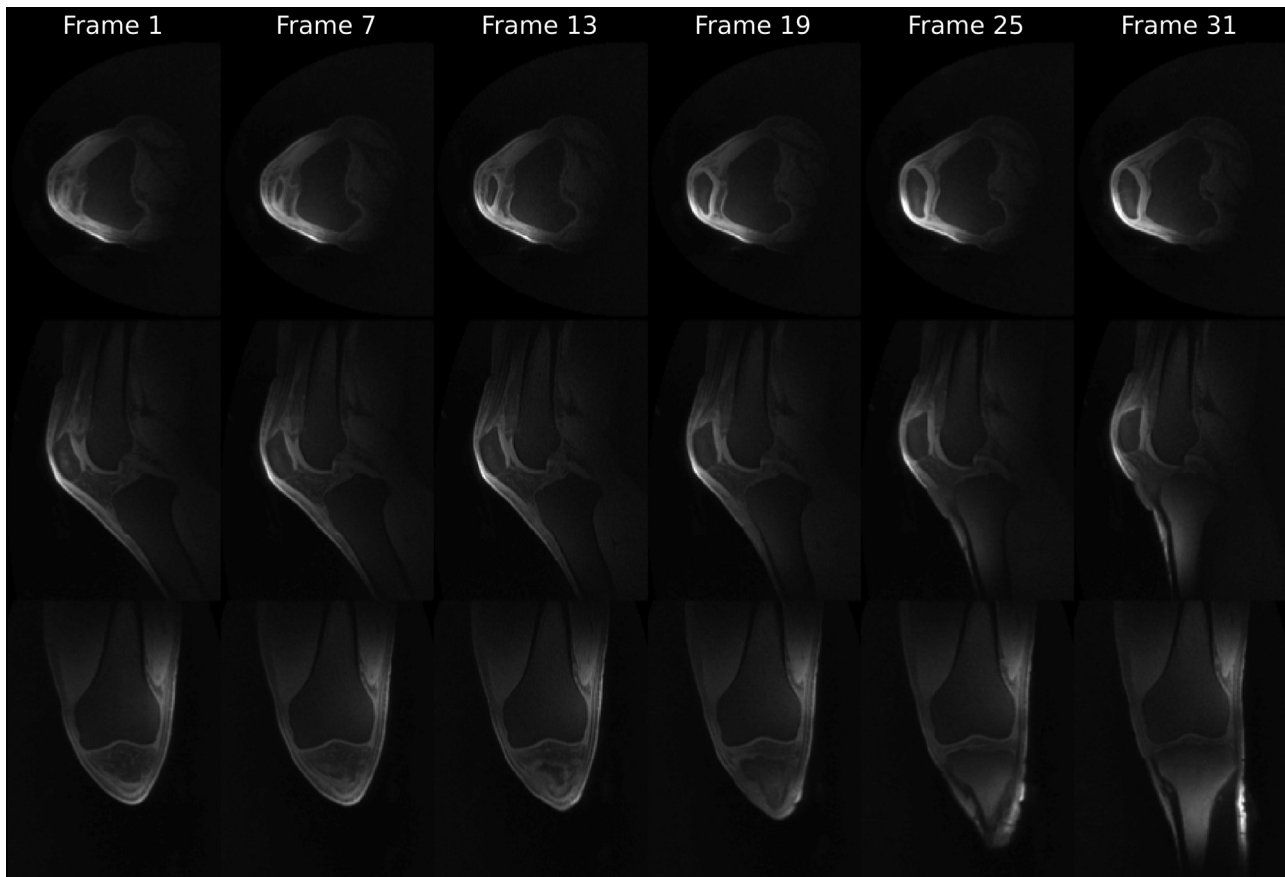
Figure 7. Six selected frames illustrating the extension portion of one passive knee extension-flexion cycle acquired in axial (top row), sagittal (middle row) and coronal (bottom row) planes. Isotropic images were acquired continuously over 48 minutes with a 3D radial UTE imaging sequence. A video showing all frames acquired continuously is available (Video 4).

baseplate through which the lower leg can move; achievable knee moments under loaded conditions were comparable [14,15]. Importantly, these magnitudes of knee motion and loading are encountered during the stance phase of gait [25], underscoring their physiological relevance. Furthermore, the versatility of the device allows for dynamic MRI data to be acquired with the patient in supine or prone position, and during volitional, loaded motion driven either by the quadriceps or the hamstring. Such versatility is useful for accommodating patient preference/comfort and for performing in vivo investigations of knee tissues during different joint motion and loading conditions. Also, the distal position of the gearbox/motorized system connection allows changing between passive and active motion types, quadriceps and hamstring-driven motion, and load magnitudes between image acquisitions without displacing the patient. Finally, by simply customizing the baseplate design, the device can be adapted for use with other MRI systems with different bore diameters and patient table dimensions.

To our knowledge, no prior report has evaluated the participant experience using MRI-safe knee motion and/or loading devices. We deemed it important to characterize the participant experience in healthy individuals prior to extending use of the device to older persons and patients with musculoskeletal knee conditions who may experience worsening symptoms with motion and loading. While some pain and discomfort was experienced in the index quadriceps muscle by a sub-group of participants, levels were generally classified as low or mild. As expected, due to lengthy active protocols (90 seconds), all participants reported some level of physical exertion for all protocols. Furthermore, visual assessment of Figure 5 suggested a trend toward increasing levels of pain, discomfort and physical exertion with increasing speeds and loads. The presence of quadriceps pain and discomfort in some participants was not surprising, and was likely directly due to knee loading (i.e., exercise-induced muscular pain/discomfort) rather than the device itself. The subjective experience during knee loading is participant-specific and influenced by several factors such as previous exposure to knee loading protocols (i.e., resistance training), as well as knee muscle strength and endurance. Accordingly, it is impossible to avoid muscular pain/discomfort entirely for some individuals. Ultimately, this
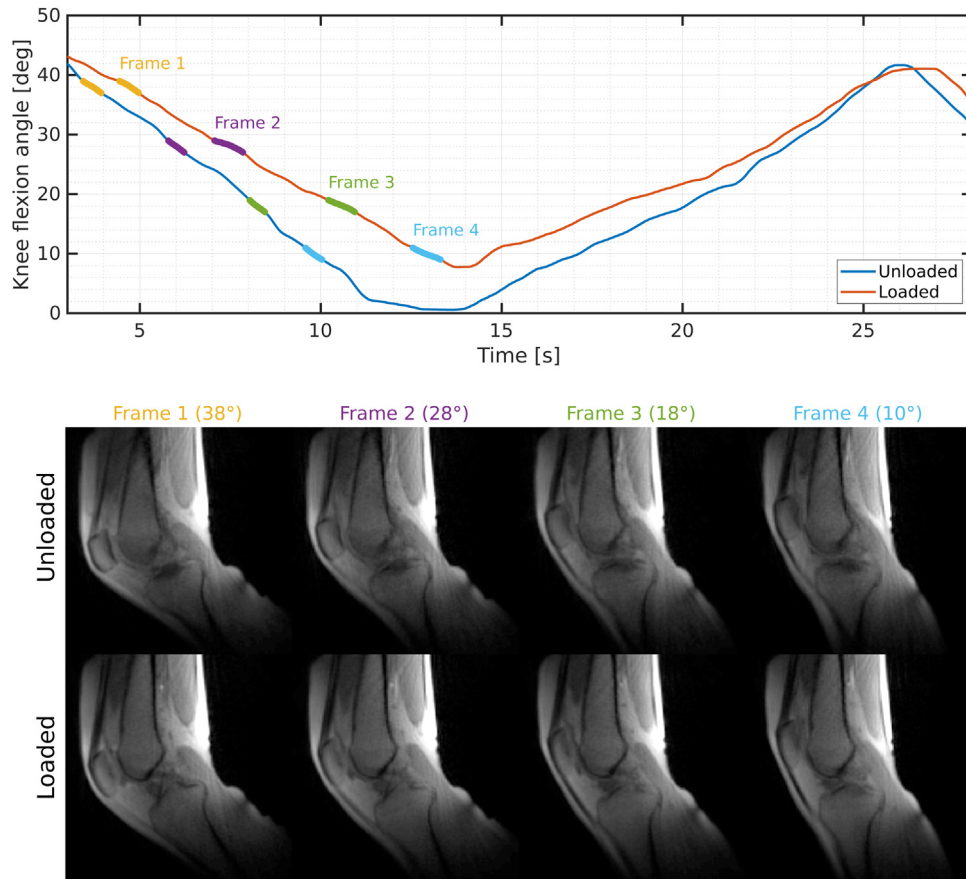
Figure 8. Knee angular data collected with a rotary encoder during active, unloaded and loaded (15 kg), knee extension-flexion cycles, with color-coded regions from where the data were extracted to reconstruct each of the four frames at knee flexion angles of 38°, 28°, 18° and 10°, respectively (top); the corresponding frames, acquired for the unloaded and loaded conditions using 2D single-echo, radial GRE imaging, are shown underneath.

knowledge can be applied to develop protocols that minimize pain and discomfort.

The device allowed for MRI acquisition during passive and active knee motion. Naturally, the slow, passive motion allowed for higher resolution images to be acquired using both radial and Cartesian trajectories. Despite this, data acquired using the latter suffered from minor aliasing artifacts, possibly caused by the knee motion itself or field of view limitations. Consequently, radial imaging sequences were chosen for all other scans due to their inherent robustness against motion and aliasing artifacts [26]. Furthermore, the device allowed passive knee motion stable enough for continuous 3D acquisition with isotropic resolution using a radial UTE sequence. Since this imaging sequence enables retrospective reformatting of dynamic MRI data to any orientation, it may permit more accurate 3D segmentation and tissue tracking during joint motion compared to 2D imaging for which outcomes may be influenced by through-slice tissue shifts [27]. In addition, position-dependent increases in signal intensity could be noticed in some tissues; for example, in the patellar

tendon as knee flexion angles increased (see Figures 6, 7 and 8) due to magic angle effects [28], and in the tibia as knee flexion angles decreased (see Figures 6 and 7) due to reduced fat saturation efficacy [29]. Finally, data acquired during faster muscle-driven (active) motions were limited to a single sagittal slice acquired with reduced temporal resolution of 0.5 seconds per frame; however, this enabled acquisition of dynamic data under conditions that were more physiologically relevant. By applying recent advances in real-time MRI [30,31] and compressed sensing [32], it should be possible to acquire images with higher temporal resolution to resolve faster, and therefore, more physiologically relevant volitional motions.

Mention of further device applications and potential use of dynamic data beyond qualitative visualization is warranted. Currently, dynamic MRI is typically performed using one of three approaches [11,33]: stepwise acquisition with a change in the position of the joint between each acquisition; motion-triggered acquisition that requires multiple repetitions of the same motion cycle (i.e., CINE MRI); or specialized

acquisition sequences that facilitate real-time MRI during continuous joint motion requiring no repetition. Although all imaging data presented in this manuscript were sampled using continuous dynamic MRI, the device can be used with all three of the aforementioned approaches. For instance, since the device allows to lock the knee in specific knee flexion angles, it can be used for stepwise acquisition of static images with manual changes in knee angle between each acquisition. This can be useful for acquiring high-resolution images of joint structures that could otherwise not be sufficiently temporally and spatially resolved when imaging continuous motion. Nonetheless, the novel device allows for slow, continuous, passive knee motion (i.e., as slow as 1°/min), likely overcoming the need for stepwise, static image acquisition. Moreover, reconstruction of image frames based on the rotary encoder data ensures matching knee angles for comparing data from different trials, sessions or conditions; and may be used to combine data from multiple motion cycles to enable CINE imaging [17]. However, this possibility remains subject to future studies as standard CINE imaging may represent a suboptimal option for populations with musculoskeletal disorders as the need for repetitive and often lengthy motion (up to 2 minutes) may be unfeasible due to symptoms (e.g., pain, weakness) [13], especially during volitional, loaded knee motion. Another alternative is real-time MRI, which acquires a time series of single image slices with reduced spatial resolution and volume coverage in only one motion cycle [1]. As dynamic MRI acquisition methods (and times) continue to improve, use of such multipurpose knee motion and loading devices could prove indispensable for facilitated evaluation and quantification of in vivo musculoskeletal dynamics in healthy and pathological populations, including functional joint anatomy, tissue deformation (or strain), morphology/morphometry and relaxation parameter mapping [12].

This study had some limitations. First, the device can only be used with surface coils or flex coils. Second, the maximum speed of passive knee motion is limited to 10.5°/min due to the current design and capacity of the motorized system. Third, load magnitude and direction during knee motion were not validated (e.g., using load cells). Such a validation is required in future work to enable detailed biomechanical characterizations of joint loading when using the device. Fourth, the participant experience using the knee motion/loading device was characterized for healthy males only. It remains to be determined whether device use is also well tolerated in other populations, including older persons and patients with musculoskeletal knee conditions. Fifth, device functionality with participants in prone position and during active, hamstring-driven motion was confirmed outside of the MRI scanner only; thus, no imaging data were presented for these conditions. Finally, demonstrating device use for advanced dynamic MRI applications (e.g., CINE, morphology/relaxometry measurements) was outside the scope of this work.

5 Conclusion

A novel multipurpose device for guided knee motion and loading during dynamic MRI was developed. Preliminary data demonstrated that use of the device was well tolerated in healthy individuals and suitable for acquiring high quality imaging data during different motion and loading conditions. In future work, this device could be used to further our understanding of physiological and pathological joint mechanics, and to evaluate various musculoskeletal knee conditions.

Acknowledgements

Appendix. List of materials used to build the different components of the knee motion/loading device.

Identifier	Description	Material (or item #)	Manufacturer
MRI-safe materials			
A	Baseplate	POM	Grünberg Kunststoffe
	Pins	PLA filament	BASF Innofil3D *
B	Cut-outs for coil plugs	----------------	----------------
C	Proximal pillow blocks	POM	Grünberg Kunststoffe
		PLA filament	BASF Innofil3D *
	Ball bearings	Ultra-high-molecular-weight	MISUMI
	Axles	polyethylene + Soda-lime glass	
	30-toothed sprockets	Fiberglass	Fibrolux
		Onyx filament	
			Mark3D *

Identifier	Description	Material (or item #)	Manufacturer
D	Thigh strap attachments	PLA filament	BASF Innofil3D *
	Thigh strap/padding	Nylon (Velcro)/foam	Fastech/CERV
E	Rotary encoder attachments	Onyx filament	Mark3D *
F	Rotary encoder	Polyether ether ketone (encasing)	Micronor
G	Thigh positioning wedge	PLA filament	BASF Innofil3D *
H	Leg support	POM	Grünberg Kunststoffe
I	Ankle rest	PLA filament	BASF Innofil3D *
	Ankle strap/padding	Nylon (Velcro)/foam	Fastech/CERV
J	Distal pillow blocks	Onyx filament	Mark3D *
	Ball bearings	Plastic + Glass	MISUMI
	30-toothed sprockets	Onyx filament	Mark3D *
K	Drive axle shafts	Fiberglass	Fibrolux
	Bracing disks	Onyx filament	Mark3D *
L	44-toothed circular gear	Onyx filament	Mark3D *
M	Belts	Polyurethane + Kevlar	Zahnriemen24
N	Belt clamps	PLA filament	BASF Innofil3D *
O	Gearbox	POM	Grünberg Kunststoffe
	Axles	Fiberglass	Fibrolux
P	Proximal, upper, 30-toothed circular gear	Onyx filament	Mark3D *
	Ball bearings	Plastic + Glass	Reely
Q	Proximal, lower, 30-toothed circular gear	Onyx filament	Mark3D *
	Ball bearings	Plastic + Glass	Reely
R	Distal, 44-toothed circular gear	Onyx filament	Mark3D *
	Ball bearings	Plastic + Glass	Reely
S	21-toothed linear gear	Onyx filament	Mark3D *
		Fiberglass	Fibrolux
T	Weight plates	PVC + cement mix	Gorilla Sports
U	Gearshift	POM	Grünberg Kunststoffe
		PLA filament	BASF Innofil3D *
	Ball bearings	Plastic + Glass	Reely
V	Locking pin	PLA filament	BASF Innofil3D *
		Fiberglass	Fibrolux
W	Inflatable air cushions	Resin + fiberglass	PChero
X	Air cushion connector	PLA filament	BASF Innofil3D *
Y	Compression platform	POM	Grünberg Kunststoffe
		PLA	BASF Innofil3D *
Z	Compression platform adapter	PLA filament	BASF Innofil3D *
		Fiberglass	Fibrolux
Other materials	Air tube *(joins device to motor assembly)*	Polyurethane (maximum pressure: 0.8 MPa)	MISUMI
	Screws	Polyamide (nylon)	Frantos
	Adhesives	Urethane methacrylate (UV632)	Permabond
		Acrylate (Vitralit 7041)	Panacol
Motor assembly materials (located outside the MR environment)			
I	Control box	Aluminum	MISUMI
		Acrylic glass	Grünberg Kunststoffe
II	Control panel	PLA filament	BASF Innofil3D *
		1.3" SPI Serial 128x64 OLED module for Arduino	SainSmart
III	Microcontroller	Arduino Mega 2560	Arduino

Identifier	Description	Material (or item #)	Manufacturer
IV	Digital stepper driver	DM542T	Stepperonline
V	Linear actuator †	Unspecified (load capacity: 750 N; stroke length: 100 mm)	Justech
	Stepper motor	Unspecified (current: 1.5 A; step angle: 1.8°)	MVPower
VI	Piston rod	Fiberglass	Fibrolux
	Compression plate	PVC	Grünberg Kunststoffe
VII	Inflatable air cushions	Resin + fiberglass	PChero
VIII	Bulb air pump	Polyurethane	PChero
	Y-connector	PBT (USYL6)	MISUMI

Note: POM = polyoxymethylene; PLA = polylactic acid; PVC = polyvinyl chloride; PBT = polybutylene terephthalate.

* indicates custom 3D-printing.

† indicates modified design: the original motor was replaced with a stepper motor.

Appendix A Supplementary data

Supplementary data associated with this article can be found, in the online version, at https://doi.org/10.1016/j.plantsci.2004.08.011.

References

[1] Shapiro LM, Gold GE. MRI of weight-bearing and movement. Osteoarthr Cartil 2012;20:69–78.

[2] Draper CE, Besier TF, Fredericson M, et al. Differences in patellofemoral kinematics between weight-bearing and non-weight-bearing conditions in patients with patellofemoral pain. J Orthop Res 2011;29:312–7.

[3] Shellock FG, Mink JH, Deutsch AL, et al. Patellofemoral joint: Identification of abnormalities with active-movement. 'unloaded' versus 'loaded' kinematic MR imaging techniques. Radiology 1993;188:575–8.

[4] McWalter EJ, Hunter DJ, Wilson DR. The effect of load magnitude on three-dimensional patellar kinematics in vivo. J Biomech 2010;43:1890–7.

[5] Powers CM, Ward SR, Fredericson M, et al. Patellofemoral kinematics during weight-bearing and non-weight-bearing knee extension in persons with lateral subluxation of the patella?: A preliminary study. J Orthop Sports Phys Ther 2003;33:677–85.

[6] D'Entremont AG, Nordmeyer-Massner JA, Bos C, et al. Do dynamic-based MR knee kinematics methods produce the same results as static methods? Magn Reson Med 2013;69:1634–44.

[7] Andriacchi TP, Mundermann A, Lane Smith R, et al. A framework for the in vivo pathomechanics of osteoarthritis at the knee. Ann Biomed Eng 2004;32:447–57.

[8] DeFrate LE, Kim-Wang SY, Englander ZA, et al. Osteoarthritis year in review 2018: mechanics. Osteoarthr Cartil 2019;27:392–400.

[9] Davis IS, Powers CM. Patellofemoral pain syndrome: proximal, distal, and local factors, an international retreat. April 30-May 2, 2009, Fells Point, Baltimore, MD. J Orthop Sport Phys Ther 2010;40:A1–16.

[10] Leal A, Andrade R, Flores P, et al. Unilateral anterior knee pain is associated with increased patellar lateral position after stressed lateral translation. Knee Surgery, Sport Traumatol Arthrosc 2020;28:454–62.

[11] Garetier M, Borotikar B, Makki K, et al. Dynamic MRI for articulating joint evaluation on 1.5 T and 3.0 T scanners: setup, protocols, and real-time sequences. Insights Imaging 2020;11:66.

[12] Jerban S, Chang EY, Du J. Magnetic resonance imaging (MRI) studies of knee joint under mechanical loading: Review. Magn Reson Imaging 2020;65:27–36.

[13] Borotikar B, Lempereur M, Lelievre M, et al. Dynamic MRI to quantify musculoskeletal motion: A systematic review of concurrent validity and reliability, and perspectives for evaluation of musculoskeletal disorders. PLoS One 2017;12:e0189587.

[14] Silder A, Westphal CJ, Thelen DG. A magnetic resonance-compatible loading device for dynamically imaging shortening and lengthening muscle contraction mechanics. J Med Device 2009;3, http://dx.doi.org/10.1115/1.3212559.

[15] Westphal CJ, Schmitz A, Reeder SB, et al. Load-dependent variations in knee kinematics measured with dynamic MRI. J Biomech 2013;46:2045–52.

[16] American College of Radiology Committee on MR Safety. ACR manual on MR safety, https://www.acr.org/-/media/ACR/Files/Radiology-Safety/MR-Safety/Manual-on-MR-Safety.pdf (2020).

[17] Krämer M, Herrmann KH, Biermann J, et al. Retrospective reconstruction of cardiac cine images from golden-ratio radial MRI using one-dimensional navigators. J Magn Reson Imaging 2014;40:413–22.

[18] Winkelmann S, Schaeffter T, Koehler T, et al. An optimal radial profile order based on the golden ratio for time-resolved MRI. IEEE Trans Med Imaging 2007;26:68–76.

[19] Krämer M, Herzau B, Reichenbach JR. Segmentation and visualization of the human cranial bone by T2* approximation using ultra-short echo time (UTE) magnetic resonance imaging. Z Med Phys 2020;30:51–9.

[20] Krämer M, Maggioni MB, Brisson NM, et al. T1 and T2* mapping of the human quadriceps and patellar tendons using ultra-short echo-time (UTE) imaging and bivariate relaxation parameter-based volumetric visualization. Magn Reson Imaging 2019;63:29–36.

[21] Glover GH, Pauly JM. Projection reconstruction techniques for reduction of motion effects in MRI. Magn Reson Med 1992;28:275–89.

[22] Uecker M, Hohage T, Block KT, et al. Image reconstruction by regularized nonlinear inversion - Joint estimation of coil sensitivities and image content. Magn Reson Med 2008;60:674–82.

[23] Uecker M, Ong F, Tamir JI, et al. Berkeley Advanced Reconstruction Toolbox. In: Proceedings of the 23rd Annual Meeting of the International Society for Magnetic Resonance in Medicine. Toronto, 2015, 2486.

[24] Zwart NR, Johnson KO, Pipe JG. Efficient sample density estimation by combining gridding and an optimized kernel. Magn Reson Med 2012;67:701–10.

[25] Silder A, Heiderscheit B, Thelen DG. Active and passive contributions to joint kinetics during walking in older adults. J Biomech 2008;41:1520–7.

[26] Block KT, Chandarana H, Milla S, et al. Towards routine clinical use of radial stack-of-stars 3D gradient-echo sequences for reducing motion sensitivity. J Korean Soc Magn Reson Med 2014;18:87–106.

[27] Zaitsev M, Maclaren J, Herbst M. Motion artefacts in MRI: a complex problem with many partial solutions. J Magn Reson Imaging 2015;42:887–901.

[28] Bydder M, Rahal A, Fullerton GD, et al. The magic angle effect: A source of artifact, determinant of image contrast, and technique for imaging. J Magn Reson Imaging 2007;25:290–300.

[29] Delfaut EM, Beltran J, Johnson G, et al. Fat suppression in MR imaging: Techniques and pitfalls. Radiographics 1999;19:373–82.

[30] Frahm J, Voit D, Uecker M. Real-time magnetic resonance imaging: Radial gradient-echo sequences with nonlinear inverse reconstruction. Invest Radiol 2019;54:757–66.

[31] Uecker M, Zhang S, Voit D, et al. Real-time MRI at a resolution of 20 ms. NMR Biomed 2010;23:986–94.

[32] Lustig M, Donoho D, Pauly JM. Sparse MRI: The application of compressed sensing for rapid MR imaging. Magn Reson Med 2007;58:1182–95.

[33] Shellock FG. Functional assessment of the joints using kinematic magnetic resonance imaging. Semin Musculoskelet Radiol 2003;7:249–76.